Huygens wavefront tracing: A robust alternative to ray tracing

Paul Sava and Sergey Fomel, Stanford University

SUMMARY

Traveltime computation is widely used in seismic modeling, imaging and velocity analysis. The two most commonly used methods are ray tracing and numerical solutions to the eikonal equation. Eikonal solvers are fast and robust, but are limited to computing only the first arrival traveltimes. Ray tracing can compute multiple arrivals, but lacks the robustness of eikonal solvers. Here, we propose a robust and complete method of traveltime computation. It is based on a system of partial differential equations equivalent to the eikonal equation, but formulated in the ray coordinate system. We use a first-order discretization scheme that is interpreted very simply in terms of Huygens' principle. The method has proved to be a robust alternative to conventional ray tracing, while being faster and having a better ability to penetrate shadow zones.

INTRODUCTION

Though traveltime computation is widely used in seismic modeling and imaging, attaining sufficient accuracy without compromising speed and robustness is problematic. Moreover, there is no easy way to obtain the traveltimes corresponding to the multiple arrivals that appear in complex velocity media.

The tradeoff between speed and accuracy becomes apparent in the choice between the two most commonly used methods, ray tracing and numerical solutions to the eikonal equation. Other methods reported in the literature, for example dynamic programming (Moser, 1991), wavefront construction (Vinje et al., 1993), etc. are less common in practice (Audebert et al., 1997).

Eikonal solvers provide a relatively fast and robust method of traveltime computations (Vidale, 1990; van Trier and Symes, 1991; Popovici and Sethian, 1997). They also avoid the problem of traveltime interpolation to a regular grid which imaging applications require. However, the conventional eikonal solvers compute first-arrival traveltimes and lack the important ability to track multiple arrivals. In complex velocity structures, the first arrival does not necessarily correspond to the most energetic wave, and other arrivals can be crucially important for accurate modeling and imaging (Geoltrain and Brac, 1993; Gray and May, 1994).

On the other hand, one-point ray tracing can compute multiple arrivals with great accuracy. Unfortunately, it lacks the robustness of eikonal solvers. Increasing the accuracy of ray tracing in the regions of complex velocity variations raises the cost of the method and makes it prohibitively expensive for routine large-scale applications. Mathematically, ray tracing amounts to a numerical solution of the initial value problem for a system of ordinary differential equations (Červený, 1987). These ray equations describe characteristic lines of the eikonal partial differential equation.

Here, we propose a different approach to traveltime computation that is robust, and has the ability to find multiple arrival traveltimes. The theoretical construction is based on a system of partial differential equations, equivalent to the eikonal equation, but formulated in the ray coordinate system. Unlike eikonal solvers, our method produces the output in ray coordinates. Unlike ray tracing, it is computed by a numerical solution of partial differential equations. We show that the first-order discretization scheme has a remarkably simple interpretation in terms of Huygens' principle, and propose a *Huygens wavefront tracing* (HWT) scheme as a robust alternative to conventional ray tracing. Numerical examples demonstrate the following properties of the method: stability in media with strong and sharp lateral velocity variations, better coverage of shadow zones, and increased speed compared to paraxial ray tracing.

CONTINUOUS THEORY

The 3-D eikonal equation, governing the traveltimes from a fixed source in isotropic heterogeneous media, has the form

$$\left(\frac{\partial \tau}{\partial x}\right)^2+\left(\frac{\partial \tau}{\partial y}\right)^2+\left(\frac{\partial \tau}{\partial z}\right)^2=\frac{1}{v^2(x,y,z)}\;. \tag{1}$$

Here x, y, and z are spatial coordinates, τ is the traveltime (eikonal), and v stands for the velocity field. Constant-traveltime surfaces in the traveltime field $\tau(x,y,z)$, constrained by equation (1) and appropriate boundary conditions, correspond to wavefronts of the propagating wave. Additionally, each point on a wavefront can be parameterized by two arbitrarily chosen ray parameters γ and ϕ.

For a point source, γ and ϕ can be chosen as the initial ray angles at the source. Zhang (1993) shows that γ and ϕ as a function of spatial coordinates satisfy the simple partial differential equations:

$$\begin{aligned}\frac{\partial \tau}{\partial x}\frac{\partial \gamma}{\partial x}+\frac{\partial \tau}{\partial y}\frac{\partial \gamma}{\partial y}+\frac{\partial \tau}{\partial z}\frac{\partial \gamma}{\partial z}&=0\;,\\ \frac{\partial \tau}{\partial x}\frac{\partial \phi}{\partial x}+\frac{\partial \tau}{\partial y}\frac{\partial \phi}{\partial y}+\frac{\partial \tau}{\partial z}\frac{\partial \phi}{\partial z}&=0\;.\end{aligned} \tag{2}$$

Equations (2) merely expresses the fact that in an isotropic medium, rays are locally orthogonal to wavefronts.

It is important to note that for complex velocity fields, τ, γ, and ϕ as functions of x, y, and z become multi-valued. In this case, the multi-valued character of the ray parameters, γ and ϕ corresponds to the situation where more than one ray from the source passes through a particular point $\{x,y,z\}$ in the subsurface. This situation presents a very difficult problem when equations (1) and (2) are solved numerically. Typically, only the first-arrival branch of the traveltime is picked in the numerical calculation. The ray tracing method is free from that limitation because it operates in the ray coordinate system. Ray tracing computes the traveltime τ and the corresponding ray positions x,y,z for a fixed pair of ray parameters (γ and ϕ).

Since $x(\tau,\gamma,\phi)$, $y(\tau,\gamma,\phi)$ and $z(\tau,\gamma,\phi)$ are uniquely defined for arbitrarily complex velocity fields, we can now make the following mathematical transformation. Considering equations (1) and (2) as a system, and applying the general rules of calculus, we can transform this system by substituting the inverse functions $x(\tau,\gamma,\phi)$, $y(\tau,\gamma,\phi)$ and $z(\tau,\gamma,\phi)$ for the original fields τ, γ, and ϕ. The resultant expressions take the form

$$\left(\frac{\partial x}{\partial \tau}\right)^2+\left(\frac{\partial y}{\partial \tau}\right)^2+\left(\frac{\partial z}{\partial \tau}\right)^2=v^2\,(x,y,z) \tag{3}$$

and

$$\begin{aligned}\frac{\partial x}{\partial \tau}\frac{\partial x}{\partial \gamma}+\frac{\partial y}{\partial \tau}\frac{\partial y}{\partial \gamma}+\frac{\partial z}{\partial \tau}\frac{\partial z}{\partial \gamma}&=0\;,\\ \frac{\partial x}{\partial \tau}\frac{\partial x}{\partial \phi}+\frac{\partial y}{\partial \tau}\frac{\partial y}{\partial \phi}+\frac{\partial z}{\partial \tau}\frac{\partial z}{\partial \phi}&=0\;.\end{aligned} \tag{4}$$

Comparing equations (3) and (4) with the original system (1-2) shows that equations (3) and (4) again represent the dependence of ray coordinates and Cartesian coordinates in the form of partial differential equations. However, the solutions of system (3-4) are better behaved and have a unique value for every τ, γ, and ϕ. We could also compute

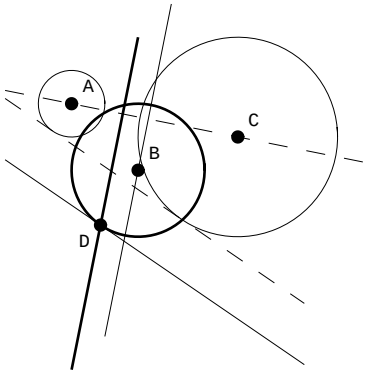

Figure 1: A geometrical updating scheme for the 2-D HWT in the physical domain. Three points on the current wavefront (A, B, and C) are used to compute the position of the D point. The bold lines represent the 2-D versions of equations (5) and (7). The tangent to circle B at point D is parallel to the common tangent of circles A and C.

these values with the conventional ray tracing. However, the ray-tracing approach is based on a system of ordinary differential equations, which represents a very different mathematical model.

We use equations (3) and (4) as the basis of our wavefront tracing algorithm. The next section discusses the discretization of the partial differential equations and the physical interpretation we have given to the scheme.

DISCRETIZATION SCHEME AND HUYGENS' PRINCIPLE

A natural first-order discretization scheme for equation (3) leads to the difference equation

$$\left(x_{j+1}^{i,k}-x_j^{i,k}\right)^2+\left(y_{j+1}^{i,k}-y_j^{i,k}\right)^2+\left(z_{j+1}^{i,k}-z_j^{i,k}\right)^2=\left(r_j^{i,k}\right)^2\ , \tag{5}$$

where the index i corresponds to the ray parameter γ, k corresponds to the ray parameter ϕ, j corresponds to the traveltime τ, $r_j^{i,k}=\triangle\tau\, v_j^{i,k}$, $\triangle\tau$ is the increment in time, and $v_j^{i,k}$ is the velocity at the $\{i,k,j\}$ grid point. It is easy to notice that equation (5) simply describes a sphere with the center at $\{x_j^{i,k}, y_j^{i,k}, z_j^{i,k}\}$ and the radius $r_j^{i,k}$. This sphere is, of course, the wavefront of a secondary Huygens source.

This observation suggests that we apply the Huygens' principle directly to find an appropriate discretization for equation (4). Let us consider a family of Huygens spheres, centered at the points along the current wavefront (τ). Mathematically, this family is described by an equation analogous to (5), as follows:

$$\left[x-x(\gamma,\phi)\right]^2+\left[y-y(\gamma,\phi)\right]^2+\left[z-z(\gamma,\phi)\right]^2=r^2(\gamma,\phi)\ . \tag{6}$$

Here the ray parameters γ and ϕ serve as the parameters that distinguish a particular Huygens' source. According to the Huygens' principle, the next wavefront corresponds to the envelope of the wavefront family. To find the envelope condition, we can simply differentiate both sides of equation (6) with respect to the family parameter, γ or ϕ.

To complete the discretization, we can represent the γ and ϕ derivatives by a centered finite-difference approximation. This representation yields the scheme

$$\left(x_j^{i,k}-x_{j+1}^{i,k}\right)\left(x_j^{i+1,k}-x_j^{i-1,k}\right)\quad+$$

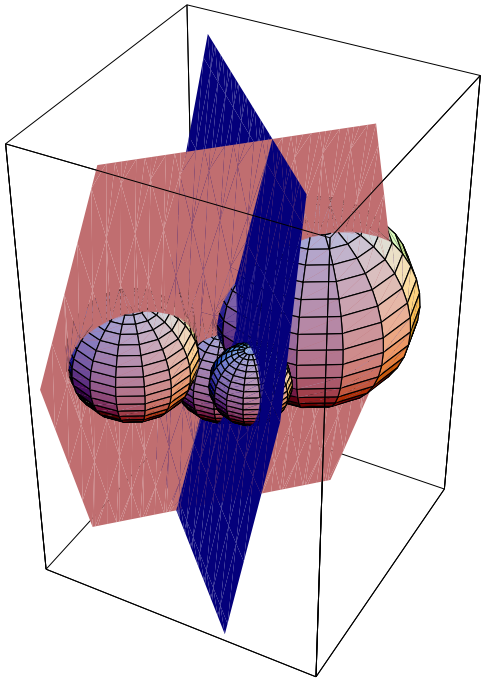

Figure 2: A geometrical updating scheme for the 3-D HWT in the physical domain. Five points on the current wavefront, represented by the five spheres, not all visible, with radii defined by the velocities at the corresponding points of the wavefront, are used to compute a point on the next wavefront. The sphere in the middle represents equation (5), and the planes represent equations (7) and (8).

$$\begin{aligned}\left(y_j^{i,k}-y_{j+1}^{i,k}\right)\left(y_j^{i+1,k}-y_j^{i-1,k}\right)\quad+\\ \left(z_j^{i,k}-z_{j+1}^{i,k}\right)\left(z_j^{i+1,k}-z_j^{i-1,k}\right)\quad=\\ r_j^{i,k}\left(r_j^{i+1,k}-r_j^{i-1,k}\right)\ ,\end{aligned} \tag{7}$$

and

$$\begin{aligned}\left(x_j^{i,k}-x_{j+1}^{i,k}\right)\left(x_j^{i,k+1}-x_j^{i,k-1}\right)\quad+\\ \left(y_j^{i,k}-y_{j+1}^{i,k}\right)\left(y_j^{i,k+1}-y_j^{i,k-1}\right)\quad+\\ \left(z_j^{i,k}-z_{j+1}^{i,k}\right)\left(z_j^{i,k+1}-z_j^{i,k-1}\right)\quad=\\ r_j^{i,k}\left(r_j^{i,k+1}-r_j^{i,k-1}\right)\ .\end{aligned} \tag{8}$$

which supplements the previously found scheme (5) for a unique determination of the point $\{x_{j+1}^i, y_{j+1}^i, z_{j+1}^i\}$ on the (i,k)-th ray and the $(j+1)$-th wavefront.

Formulae (5), (7), and (8) define the update scheme for the finite difference algorithm, and Figures (1) and (2) present their geometrical interpretation.

To fill the $\{\tau,\gamma,\phi\}$ volume, the scheme needs to be initialized with one complete wavefront (around the wave source) and a bundle of boundary rays to account for the exterior of the $\gamma-\phi$ domain. This second part of the initialization can be replaced by local wavefront extrapolation. The solution to the system (5, 7, 8) has an explicit form.

EXAMPLES

This section presents two examples in which we applied the method described in the last section. The first application is on a simple Gaussian

velocity anomaly in a medium of constant velocity. We used this model to check the validity, accuracy, and stability of the Huygens wavefront tracing (HWT) method. The second example concerns the very complex Marmousi model, which is one of the most difficult benchmarks for ray tracing methods. Throughout the test, we have compared our results with those obtained with a paraxial ray tracing (PRT) program (Rekdal and Biondi, 1994) for accuracy, speed, and stability.

The Gaussian velocity anomaly

Our first example is a Gaussian negative velocity anomaly with a magnitude of 2.0 km/s in a constant velocity medium of 3.0 km/s, presented in Figure 3. The anomaly is centered at a depth of 1.0 km and has a half-width of 300 m. The source is placed on the surface directly above the anomaly, at $x = 6.0\ km$.

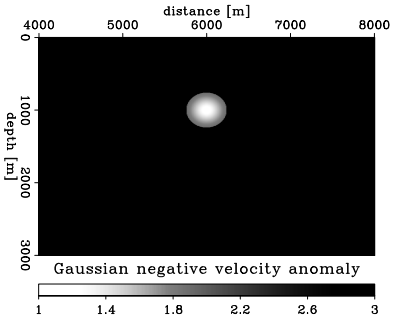

Figure 3: A Gaussian negative velocity anomaly. The background velocity is 3.0 km/s, and the maximum anomaly at the center is $-2.0\ km/s$.

We have selected this velocity model to test the way our method applies to a well known pattern of velocity variation. For such a Gaussian velocity anomaly, the rays should bend inward. The distribution of rays as obtained with the HWT method is presented in Figure 4.

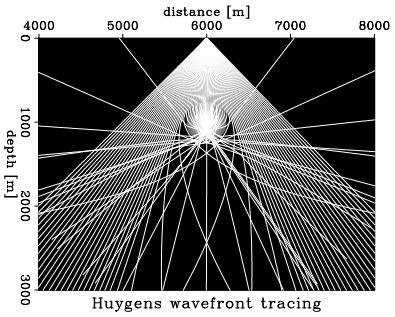

Figure 4: The rays obtained in the case of the Gaussian negative velocity anomaly. We present the rays obtained with the HWT method (right). The source is located on the surface at $x = 6.0\ km$.

The Marmousi model

In the second example, we have applied the same method to trace rays in the far more complex Marmousi Model (Versteeg and Grau, 1990) (Figure 5).

In Figure 6 we present the rays obtained on the unsmoothed (left), and smoothed (right) Marmousi model, with the HWT method (bottom), and with the PRT method (top).

As expected, the rays traced using the PRT method, which represents a more exact solution to the eikonal equation for the given velocity field, have a very rough distribution. Since this erratic result is of no use in practice, regardless of its accuracy, the only way to get a proper result is to apply the ray tracing to a smoothed velocity model (Figure **??**).

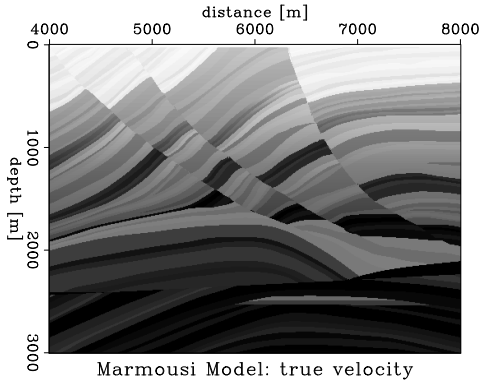

Figure 5: The Marmousi model, true velocity.

On the other hand, the result obtained with the HWT method looks a lot better, though some imperfections are still visible. For the case of the unsmoothed velocity medium, the rays have a much smoother pattern, which is less dependent on how rough the velocity model is. This feature is preserved in the case of the smoothed model (Figure **??**) where the distributions of rays displayed by the two methods are much more similar, though some differences remain (see, for example the zone around $x = 6.5\ km$, $z = 2.0\ km$).

CONCLUSIONS

We have presented a method of ray tracing based on a system of differential equations, equivalent to the eikonal equation, but formulated in the ray coordinate system. We used a first order discretization scheme, interpreted very simply in terms of the Huygens' principle. The results obtained so far, enable us to the draw the following conclusions:

1. Stability: The Huygens wavefront tracing method is more stable in rough velocity media than the paraxial ray tracing method. The increased stability results from the fact that HWT derives the points on the new wavefronts from five points on the preceding wavefront, compared to only one in the usual PRT, which also means that a certain degree of smoothing is already embedded in the method. This feature allows us to use the HWT method in media of very sharp velocity variation and still obtain results that are reasonable from a geophysical point of view.

2. Coverage: Being more stable and giving smoother rays than the PRT method, enables the HWT method to provide a better coverage of shadow zones. The idea is that since the wavefront is traced from one ray to the other, it is very easy to introduce in the code a condition to decrease the shooting angle as soon as the wavefront length exceeds a specified upper limit.

3. Speed: Both HWT and PRT methods were tested on an SGI Origin 200. In the 2-D case, the execution time for shooting 90 rays of 130 samples for each ray was 1.31 s for the PRT method and 0.22 s for the HWT method.

We are working on a 3-D implementation, and our preliminary results show that the method promises an even larger speed improvement, as compared to the 3-D ray tracing equivalents.

REFERENCES

Audebert, F., Nichols, D. E., Rekdal, T., Biondi, B., Lumley, D. E., and Urdaneta, H., 1997, Imaging complex geologic structure with

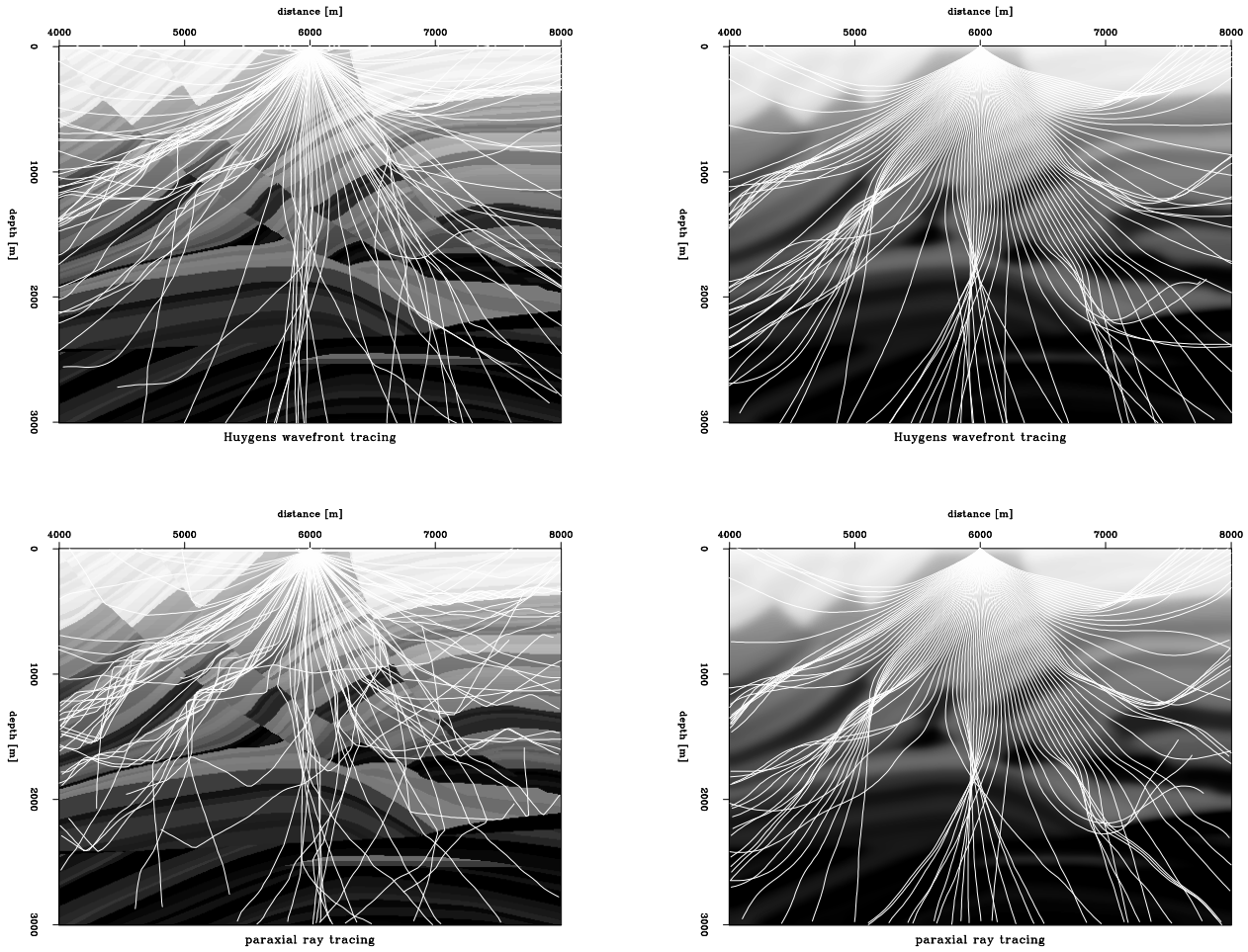

Figure 6: The rays obtained in the true velocity Marmousi model (left), and in the smoothed velocity model (right), using the HWT method (bottom), and the PRT method (top).

single-arrival Kirchhoff prestack depth migration: Geophysics, **62**, no. 5, 1533–1543.

Červený, V., 1987, Ray tracing algorithms in three-dimensional laterally varying layered structures *in* Nolet, G., Ed., Seismic Tomography:: Riedel Publishing Co., 99–134.

Geoltrain, S., and Brac, J., 1993, Can we image complex structures with first-arrival traveltime?: Geophysics, **58**, no. 4, 564–575.

Gray, S. H., and May, W. P., 1994, Kirchhoff migration using eikonal equation traveltimes: Geophysics, **59**, no. 5, 810–817.

Moser, T. J., 1991, Shortest path calculation of seismic rays: Geophysics, **56**, no. 1, 59–67.

Popovici, A. M., and Sethian, J., 1997, Three dimensional traveltime computation using the fast marching method: 67th Annual Internat. Mtg., Soc. Expl. Geophys., Expanded Abstracts, 1778–1781.

Rekdal, T., and Biondi, B., 1994, Ray methods in rough models: SEP–**80**, 67–84.

van Trier, J., and Symes, W. W., 1991, Upwind finite-difference calculation of traveltimes: Geophysics, **56**, no. 6, 812–821.

Versteeg, R., and Grau, G., 1990, Practical aspects of seismic data inversion, the Marmousi experience EAEG Workshop, 52nd EAEG Meeting, Eur. Assoc. Expl. Geophys., Proceedings of 1990 EAEG Workshop, 52nd EAEG Meeting, 1–194.

Vidale, J. E., 1990, Finite-difference calculation of traveltimes in three dimensions: Geophysics, **55**, no. 5, 521–526.

Vinje, V., Iversen, E., and Gjoystdal, H., 1993, Traveltime and amplitude estimation using wavefront construction: Geophysics, **58**, no. 8, 1157–1166.

Zhang, L., 1993, Imaging by the wavefront propagation method: Ph.D. thesis, Stanford University.